Arab J Sci Eng (2015) 40:1327–1342
DOI 10.1007/s13369-015-1629-6

RESEARCH ARTICLE - CIVIL ENGINEERING

Undrained Static Response of Loose and Medium Dense Silty Sand of Mostaganem (Northern Algeria)

Fethi Belhouari · Karim Bendani · Hanifi Missoum · Mohamed Derkaoui

Received: 27 August 2014 / Accepted: 3 March 2015 / Published online: 18 March 2015

Abstract Critical undrained shear strength of sandy soils is a fundamental parameter in stability analysis. This will help to evaluate the occurrence of flow deformation under liquefaction phenomena. A precise evaluation of the undrained liquefaction strength is very important for the design of soil structures such as earth dams, building foundations and soil densification process which can avoid catastrophic failure due to soil instability. In this work, laboratory investigation on natural and on reconstituted soil specimens of silica sands was carried out to enable the analysis of its mechanical behavior. Several concepts have been proposed by many researchers in order to characterize instability of silty sands. However, a review of studies published in the literature indicates that no clear conclusions can be drawn as to what manner the variation of fine content affects the mechanical behavior. The present paper is an attempt to experimentally describe mechanical behavior and theoretically justify such response of loose and medium dense sand by means of critical state parameters. Two distinct stress path tendencies have been shown in this study. In undrained conditions, loose samples show amplified contractive phase with fine content ranging from 0 to 30 %, while medium dense samples exhibit a contractive phase followed by a dilative phase with fine contents beyond 30 %. In this study, it has been shown that the strength of sand fabric of carrying loads becomes weaker and the critical state parameter increases with the increase in fine content leading to the reduction of normalized critical undrained shear strength.

Keywords Liquefaction · Sand–silt mixture · Density · Instability · Critical state · Undrained shear strength

F. Belhouari (✉) · K. Bendani · H. Missoum · M. Derkaoui
Department of Civil Engineering and Architecture, University Abdelhamid Ibn Badis, Mostaganem, Algeria
e-mail: Belhouari_fethi@yahoo.fr

M. Derkaoui
e-mail: dermoh2008@hotmail.com

K. Bendani · H. Missoum
Laboratory of Construction, Transports and Environment Protection (LCTPE), University Abdelhamid Ibn Badis, Route de Belhacel, BP 227, Mostaganem, Algeria
e-mail: bendanik@yahoo.fr

H. Missoum
e-mail: hanifimissoum@yahoo.fr

List of symbols

B	Skempton coefficient
CSL	Critical state line
D_r	Initial relative density
e	Global void ratio
i	Starting point of the undrained stress path (A, B or C)
i_1	Point at the peak of the undrained stress path (A_1, B_1 or C_1)
i_2	Point at the CSL of the undrained stress path (A_2, B_2 or C_2)
e_i	Void ratio at point (i)
$e_{CSL(i)}$	Void ratio at critical state at point (i)
e_{max}	Maximum void ratio
e_{min}	Minimum void ratio
F_C	Fine content (%)
G_S	Specific gravity of soil grain
C_u	Uniformity coefficient
C_c	Coefficient of curvature
p'	Effective mean stress
p'_C	Confining stress
$p'_{CSL(i)}$	Effective mean stress at critical state (undrained stress path starting from point i)

q	Deviatoric stress
$q'_{\mathrm{CSL}(i2)}$	Deviatoric stress at critical state at point ($i2$)
q_{S}	Deviatoric stress at critical state
q_{yield}	Maximum deviatoric stress
S_{ucr}	Undrained critical shear strength
$S_{\mathrm{ucr}(i)}$	Undrained critical shear strength (undrained stress path starting from point i)
$S_{\mathrm{ucr(yield)}}$	Yield shear strength
Δu	Excess pore water pressure
ε_{a}	Axial strain
D_i	Grain diameter corresponding to i % finer
σ_1	Major principal stress
σ_3	Minor principal stress
I_{p}	Plasticity index
M	Slope of critical state line in (q, p') plane
ϕ_{s}	Mobilized angle of inter-particle friction at the critical state
ψ_{CSL}	State parameter
$\psi_{\mathrm{CSL}(i)}$	State parameter at point (i)
λ_{CSL}	Critical state parameter (shearing–compressibility soil property)
Γ_{CSL}	Critical state parameter

1 Introduction

Several liquefaction flow failures are triggered by either static or cyclic loadings. Liquefaction may lead to catastrophic failure, if the shear resistance of a soil susceptible to liquefaction drops below the existing initial static load [1–3]. Olson and Stark [4] have reported many cases of static liquefaction flow failures. Critical undrained shear strength of sandy soils is a fundamental parameter in stability analysis leading to the evaluation of the occurrence of flow deformation under liquefaction phenomena. The evaluation of the undrained liquefied strength is very essential for the design of soil structures in order to predict and to avoid catastrophic failure due to soil instability.

In undrained conditions, saturated sandy soils may be vulnerable to instability due to static or dynamic loading. The region of Mostaganem where an extensive urban project as well as marine infrastructures is planned belongs to the northern part of Algeria (Fig. 1). Moreover, it lies on geological layers of vast deposits of saturated silica sand. These conditions enhance the instability phenomena. Deep strata of silica sand of the region are shown in Fig. 2. Facing soil failure phenomenon, there is a need to characterize these granular media as an engineering material.

Undrained shear strength of sandy soils may decrease sharply by either monotonic (e.g., erosion at toe of a slope under heavy rainfall, reservoir filling, rapid sediment accumulation) or dynamic (e.g., earthquake, vibration or blast). Such loadings can lead to a phenomenon of flow failure or even liquefaction; this may be manifested by large soil mass displacements such as settlement or slope failure. In saturated sandy soils, pore water pressure will be developed due to the tendency of volume contraction of the soil if the flow of water is impeded [5]. Meanwhile, a lower effective stress will be generated, followed by a reduction in soil shear strength.

As long as new in-field and laboratory observations are raised, the understanding of soil liquefaction is continuously being revised to include new soil parameters generating liquefaction. Obvious evidences had significantly affected the research trend in investigating instability of natural sandy soil deposits. The influence of fines on mechanical behavior of sand matrix soil is not yet fully understood. In this context, the present challenge is to improve fundamental research on the mechanical behavior of soils vulnerable to instability in order to obtain consensual framework to predict behavior of such soils.

Contradictory research findings [6,7] on the role of nonplastic or low plastic fines in sand matrix state that such fine

Fig. 1 Coastal region of Mostaganem (Algeria)

Fig. 2 Deep layers of silica sand of the regions of Mostaganem (Algeria)

content may either increase or decrease liquefaction vulnerability. Many contributions tried to give a physical interpretation to the influence of fines onto liquefaction behavior of sandy soils [8,9]. The well-known Chinese criteria [10] for liquefaction susceptibility identification are essentially based on in-field observations. This criterion has experienced many revisions, but it still forms the basic principles and guidelines for many codes of practices. Nevertheless, new recent evidences show some inadequacy and deviation due to the presence of fines, mainly non-plastic fines. Because of discrepancies in the research results in laboratory and in-field post-liquefaction events, many researchers agreed that such regulations should be discontinued and should be reviewed in a general context [11]. Hence, based upon conflicting results presented in the literature, the fine content in a sandy soil does not provide a unified mechanical behavioral trend in undrained conditions. Many concepts have been proposed to treat such mixtures, but this is still non-unified and sometimes controversial.

Silty sands are the most common type of soil involved in flow liquefaction events. Many static liquefaction flow failures have been detailed by Sadrekarimi [12] as well as several earthquake-induced liquefaction failure case events have been cited by Yamamuro and Lade [13]. Some types of soil with fines content may be highly susceptible to liquefaction phenomena [14]. Recently, many investigations have been performed on the effects of fine particles on the instability of sandy soils.

The stability of structures founded on liquefied soil depends on post-liquefaction of the soil shear strength. The shear strength of soils at the phase transition has an important influence for engineering design [15]. The importance of critical or residual shear strength in design of soil structures or soil densification process has been discussed by Olson and Stark [16]. Consequently, it is important to clarify the main parameters that govern substantially the shear resistance and to provide a broad understanding on contractive and dilative phases of soil behavior in undrained conditions.

In this study, a parametric study for evaluating the undrained liquefied shear strength of silty sand using critical state parameters and geotechnical properties of the mixtures is attempted. This work is conducted in the objective to investigate the effects of low plastic silty fine content on undrained liquefied shear strength of silt–sand mixture. Our main aim in this study is focused on analyzing the link between the shearing–compressibility characteristics of the mixture expressed via the critical state soil parameters and the critical undrained shear resistance. Shearing–compressibility properties of soil mixtures depend on fine content, grain distribution properties, particle mineralogy and particle shape. Critical state parameters and mean confining effective stress may be essential in evaluating instability susceptibility and the likelihood for the occurrence of a catastrophic liquefaction flow failure.

In the goal of achieving this aim, a series of monotonic undrained triaxial shear tests were performed on reconstituted saturated sand–silt mixtures specimens with specified added fine fraction ranging from 0 to 50 % with two combinations of initial relative density states (15 and 45 %) at three levels of confining effective mean stresses (100, 200 and 300 kPa).

2 Experimental Methods

Several undrained triaxial tests were carried out on natural soil collected on site and on reconstituted sand–silt mixtures specimens. The soil under investigation was collected from coastal region of Mostaganem site at two depths 1 and 4 m. The soil is a terrigenous silica sand composed mainly of quartz and feldspar, and its particle shape is more or less rounded. The grain size distribution curves of the soil at the two depths are shown in Fig. 3. The fine contents of the sand collected were found of 6.2 and 14.7 % with relative densities of 17 and 43 % at depths of 1 and 4 m, respectively. In our experiments, sand and fine particles were separated from each other and then mixed in known fractions in order to form specimens with fine contents ranging from 0 to 50 %. It can be seen here that natural soil properties are retained within the adopted fine content interval. The specific gravity of sand and silt was 2.66 and 2.64, respectively. Liquid limit and plastic limit of the silt were 16 and 10 %, respectively. It is known that liquefaction vulnerability is highly affected by the initial relative density of the soil [17,18]. In this work, loose and medium dense states have been considered. The geotechnical properties of sand on site and of reconstituted soils are presented in Table 1.

The grain size distribution curves for sand–silt mixtures under investigation are represented separately in Fig. 4. D_i

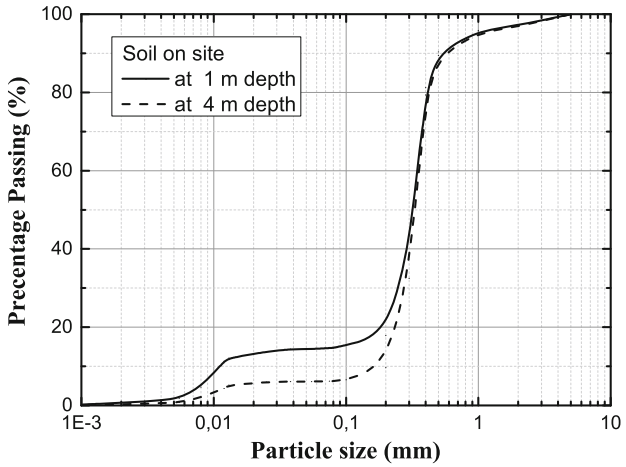

Fig. 3 Grain size distribution of sand collected on site at different depths

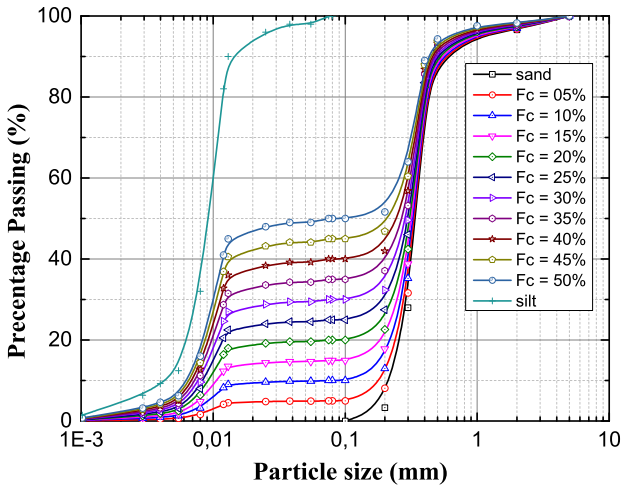

Fig. 4 Grain size distribution curves of tested specimens

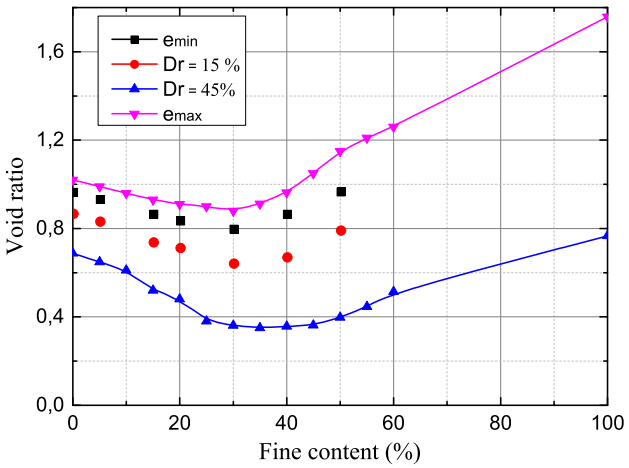

Fig. 5 Variation of maximum and minimum void ratio versus fine content

corresponds to the soil diameter at which i % of the soil weight is finer. The plasticity index of the silt I_p is 6 % with liquid limit of 16 % and according to ASTM [19] classification, the sand under study is poorly graded (SP), while the silt is inorganic (ML) and low plastic (CL).

From Table 1, it can be deducted that the variation of both indices e_{max} and e_{min} the maximum and minimum void ratio, respectively, follows the same trend. The two indices decrease with the increase of fine content till 30 %, and then, they increase beyond this value (Fig. 5). The same observation is related by Missoum et al. [20] for Chlef (Algeria) sandy soil.

2.1 Laboratory Experiment Procedures

Numerous sample reconstitution methods have been established for use in the laboratory, such as moist tamping, dry funnel pluviation and water sedimentation. Sample preparation methods affect considerably the liquefaction behavior of soils [21,22]. The reconstituted specimens under testing must be prepared in such a way to reproduce in situ soil conditions. Hence, the choice of a proper sample preparation

Table 1 Geotechnical properties of sand–silt mixtures

Material	F_C (%)	G_S	e_{min}	e_{max}	D_{10} (mm)	D_{30} (mm)	D_{60} (mm)	C_u	C_c
Sand on site (1 m depth)	14.7	2.657	0.544	0.936	0.011	0.246	0.346	31.454	15.897
Sand on site (4 m depth)	6.2	2.659	0.638	0.983	0.157	0.270	0.360	2.250	1.260
Clean sand	0	2.660	0.688	1.020	0.213	0.288	0.363	1.704	1.073
Silty sand	5	2.659	0.648	0.990	0.180	0.277	0.357	1.983	1.194
Silty sand	10	2.658	0.611	0.960	0.085	0.264	0.353	4.163	2.328
Silty sand	15	2.657	0.520	0.930	0.011	0.247	0.345	32.303	16.558
Silty sand	20	2.656	0.480	0.910	0.009	0.225	0.338	37.102	16.441
Silty sand	30	2.654	0.361	0.880	0.008	0.092	0.321	41.797	3.418
Silty sand	40	2.652	0.357	0.962	0.007	0.011	0.297	43.421	0.063
Silty sand	50	2.650	0.397	1.150	0.006	0.010	0.256	41.424	0.063

method is essential to determine the instability potential of sandy soils. Dry pluviation deposition method tends to reproduce well field performance as shown by Vaid et al. [23]. In this present study, dry funnel pluviation was used as a sample preparation method in order to replicate the soil conditions at the field.

Dry sand and silt have been mixed according to the considered different weight ratios. The samples were prepared by means of a mold consisting of two semi-cylindrical shells. The two parts of the mold can be easily joined by a hose clamp.

The samples are cylindrical in shape of 70 mm in diameter D and 140 mm in height. According to the required relative density, mass of sand–silt mixture to be put inside the mold is determined. The relative density of reconstituted sample is defined as:

$$D_{\mathrm{r}} = (e_{\max} - e) \,/\, (e_{\max} - e_{\min}) \tag{1}$$

where e is the global void ratio.

Then, the samples have been purged by carbon dioxide gas for more than 30 min and saturated by de-aired water. The saturation state is controlled by Skempton's pore water parameter B. According to ASTM [24], samples can be considered fully saturated if B is at least equal to 0.95. In all the undrained tests performed, this condition was fulfilled. In this investigation, backpressure of 100 kPa has been applied during the test experiments in order to achieve full saturation state.

Samples were isotropically consolidated at three levels of effective mean stresses of 100, 200 and 300 kPa and then subjected to undrained monotonic compression triaxial loading. A constant strain rate of 5 %/h was applied during all the tests in order to stabilize the pore water pressure build-up throughout all the samples in undrained conditions. All the tests were carried out up to 20 % axial strain.

2.2 Evaluation of Undrained Critical Shear Strength by Means of Critical State Parameters

When three saturated sand–silt mixture specimens are susceptible to liquefy at three levels of effective mean stresses, their mechanical behavior in undrained triaxial test may be illustrated by the curves shown in Fig. 6. Points A, B and C are the locations at which samples are compressed isotropically as illustrated in Fig. 6a.

In sandy soils at undrained conditions (constant volume), the effective mean stress decreases as excess pore water pressure develops. During this process, soil samples reach peak deviatoric stress q_{yield} at positions A_1, B_1 or C_1 at small axial strain ranging from 0.8 to 2 % as shown in Fig. 6b. Instability is triggered when shear stress applied on soil specimen attempts to exceed the peak deviatoric stress q_{yield} or the peak shear strength. Beyond that point, a strain softening develops in the specimen till the critical state is reached at points A_2, B_2 or C_2 on critical state line (CSL). These positions are termed critical state [25,26] or residual state [27]. Strain softening is responsible of soil instability characterized by particle arrangement and reorientation leading to soil displacement.

Undrained shear strength S_{ucr} at critical state is the minimum undrained shear strength that is mobilized after limited liquefaction occurs.

The locus of void ratio and effective mean stress p' at critical state (A_2, B_2 and C_2) on the CSL may be expressed by the following relationship,

$$e_{\mathrm{CSL}(i)} = \Gamma_{\mathrm{CSL}} - \lambda_{\mathrm{CSL}} \log\left(p'_{\mathrm{CSL}(i)}\right) \tag{2}$$

where Γ_{CSL} is mixture critical void ratio at $p' = 1$ kPa and λ_{CSL} is the slope of the CSL in $e - \log p'$ plane (Fig. 7), $e_{\mathrm{CSL}(i)}$ stands for void ratio at critical state, the subscript i

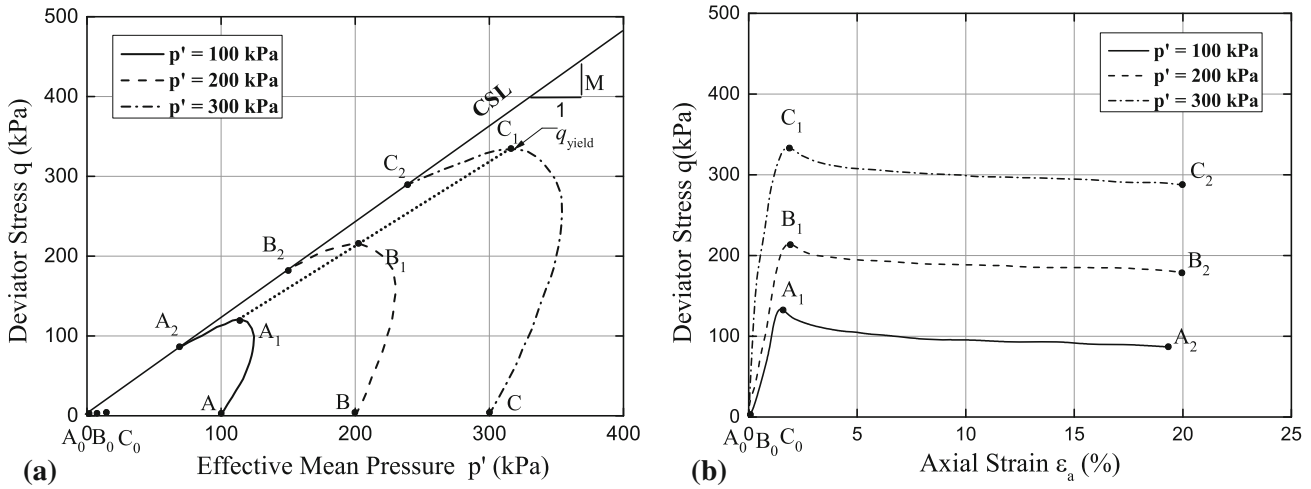

Fig. 6 **a** Idealized curves of undrained triaxial compression test results stress paths (q, p'), **b** variation of deviatoric stress versus axial strain

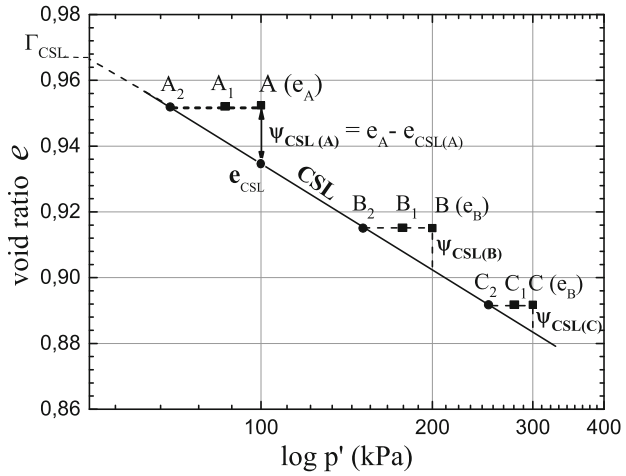

Fig. 7 Critical state representation in ($e - \log p\prime$) from undrained triaxial compression test results

denotes the starting point of the undrained stress path under consideration (A, B or C).

A relationship can be developed for evaluating normalized undrained critical shear stress S_{ucr} in terms of initial void ratio or density state and critical state parameters. According to Fig. 7, the difference in void ratio from consolidation point i, i.e., e_i to $e_{CSL(i)}$. ψ_{CSL} is the state parameter as defined by Been and Jefferies [28]. Negative values of ψ_{CSL} generally correspond to dilative and strain-hardening behavior, while positive values express the soil volume contraction and strain-softening response, and this parameter can be defined by:

$$\psi_{CSL(i)} = e_i - e_{CSL(i)} \tag{3}$$

After substitution, the following expression may be obtained:

$$\psi_{CSL(i)} = \left(\Gamma_{CSL} - \lambda_{CSL} \log\left(p'_{CSL(i2)}\right)\right) - \left(\Gamma_{CSL} - \lambda_{CSL} \log\left(p'_{CSL(i)}\right)\right) \tag{4}$$

where the subscript $i2$ is the peak point at the undrained stress path, i.e., A_2, B_2 or C_2

Again, ($\psi_{CSL(i)}$) can be written as:

$$\psi_{CSL(i)} = \lambda_{CSL} \log\left(p'_{CSL(i)} \Big/ p'_{CSL(i2)}\right) \tag{5}$$

The mean critical effective stress at critical state may be given in the following form:

$$p'_{CSL(i)} = p'_{CSL(i2)} \times 10^{(\psi_{CSL(i)}/\lambda_{CSL})} \tag{6}$$

In the framework of critical state soil mechanics theory, the following relationship can be written:

$$q_{CSL(i2)} = M \times p'_{CSL(i2)} \tag{7}$$

with M: slope of critical state line.

In the case of triaxial tests and according to Schofield and Wroth [29], the following expression can be written as:

$$\sin\phi_S = (3 \times M)/(6 + M) \tag{8}$$

where $q_{CSL(i2)}$, $p'_{CSL(i2)}$ and ϕ_S indicate the deviatoric stress $(\sigma'_1 - \sigma'_3)$, the effective mean principal stress $(\sigma'_1 + \sigma'_3)/3$ and the mobilized angle of inter-particle friction at the critical state, respectively.

$$S_{ucr(i)} = \left(q_{CSL(i2)}/2\right) \times \cos\phi_S \tag{9}$$

Finally, the relationship between the normalized undrained shear strength and the critical state parameters may be expressed in the following form:

$$\frac{S_{ucr(i)}}{p'_{CSL(i)}} = \frac{6\sin\phi_S \times \cos\phi_S}{3 - \sin\phi_S} \times 10^{(-\psi_{CSL(i)}/\lambda_{CSL})} \tag{10}$$

It is pertinent to note that Eq. (10) is obtained based on sandy soil behavior as well as the critical state from monotonic undrained triaxial tests. This expression can also be applicable to evaluate normalized shear strength S_{ucr} for contractive soils under cyclic loading, since the critical state line is independent of stress path and shear strain rate. It can be noticed that Eq. (10) depends only on the initial effective mean stress, the initial relative density (after consolidation) and the critical state parameters and does not rely on stress paths.

3 Results and Discussion

The undrained monotonic compression triaxial tests performed on sand collected on site at depths of 1 and 4 m gave the results shown in Figs. 8 and 9. As the soil gets denser with depth, it can be seen from Figs. 8 and 9, i.e., in (q, p'), (q, ε_a) and (Δu, ε_a) planes, that the soil gets stiffer with depth as well.

The natural soil specimen for both densities shows two phase tendencies, contractive and dilative; for high fine content, a contractive phase is more pronounced. A higher deviator stress at transformation phase is obtained for high relative density.

The results of the undrained monotonic compression triaxial tests carried out for different fine content ranging from 0 to 50 % at three levels of confining effective mean stresses of 100, 200 and 300 kPa and for two densities ranges (D_r = 15 and 45 %) are shown in Figs. 10, 11, 12, 13, 14, 15 and 16. During the tests, the stress paths (q, p') are recorded and represented graphically, as well as the axial strain versus the deviatoric stress q.

It can be clearly noticed that an increase in the added fines from 0 to 30 % leads to a decrease in the deviatoric stress q. This decrease comes from the role of the fines in reducing the soil dilatancy and amplifying the phase of contractancy

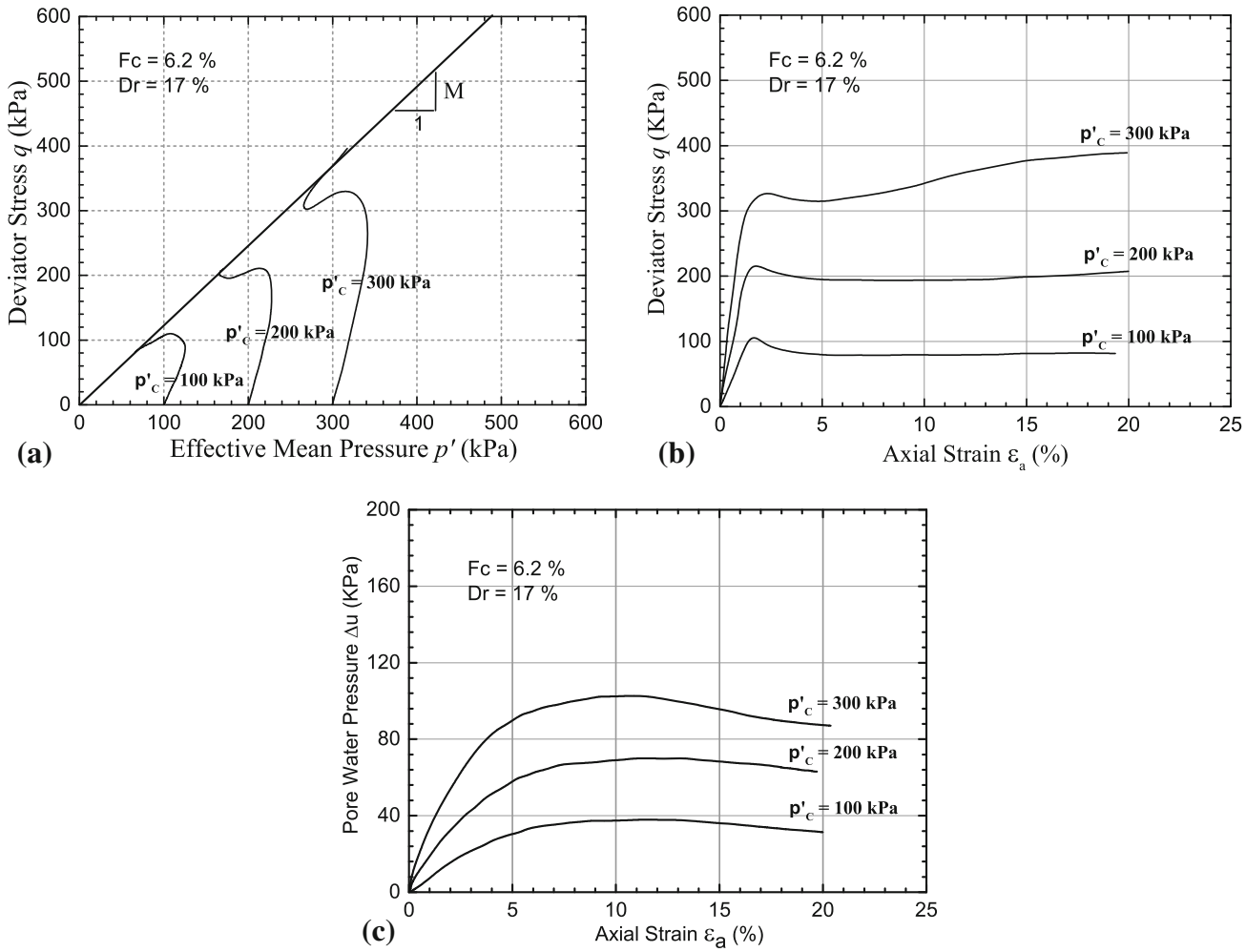

Fig. 8 Undrained compression test results on natural sand collected at 1 m depth for a confining mean stress of 100, 200 and 300 kPa

of the sand–silt mixtures. The stress path in the plane (q, p') shows clearly the role of the fines in the decrease of both the average effective pressure and the maximum deviatoric stress (Figs. 10a, 11a, 12a, 13a, 14a, 15a, 16a), and in this case, the effect of fines on the undrained behavior of the mixtures may be considered not participating in the force chain of the mixtures. Several laboratory studies reported the same observations and that the undrained shear resistance may be reduced with the increase of fine content till a threshold value of fine content [30–35].

The obtained results from the tests show two distinct stress path tendencies. Loose samples show amplified contractancy phase, while medium dense samples exhibit a contractive phase followed by a dilative phase in undrained onditions.

From Figs. 10, 11, 12, 13 and 14, it can be noticed that specimens show the same behavior under the same initial relative density and the same confining effective mean stress. The first phase of the stress paths represents the attainment of a peak deviatoric stress at small axial strain which is followed by a loss of shear strength until residual or critical shear strength is attained with no further decrease in strength. This type of behavior may be traduced by a strain softening. The rapid decline in shear strength may be associated with the soil fabric disintegration, and a consequent pore water pressure built-up will be generated as shown in Fig. 17. The pore water generation was drawn for different fine content 5, 20 and 30 % at a confining pressure of 200 kPa. It can be noticed in this figure a pronounced increase in pore water pressure generation rate with increase in fine content. The same trend has been obtained for the other considered confining pressures. This process can be manifested by a limited liquefaction.

Within the range of initial relative densities considered in this study, the peak deviatoric stress increases with the increase in confining effective mean stress for all reconstituted specimens under investigation.

When the fine fraction is over 30 %, samples exhibit dilation, there is a continuous increase in the deviatoric stress without a loss in shear strength, and this increase is due

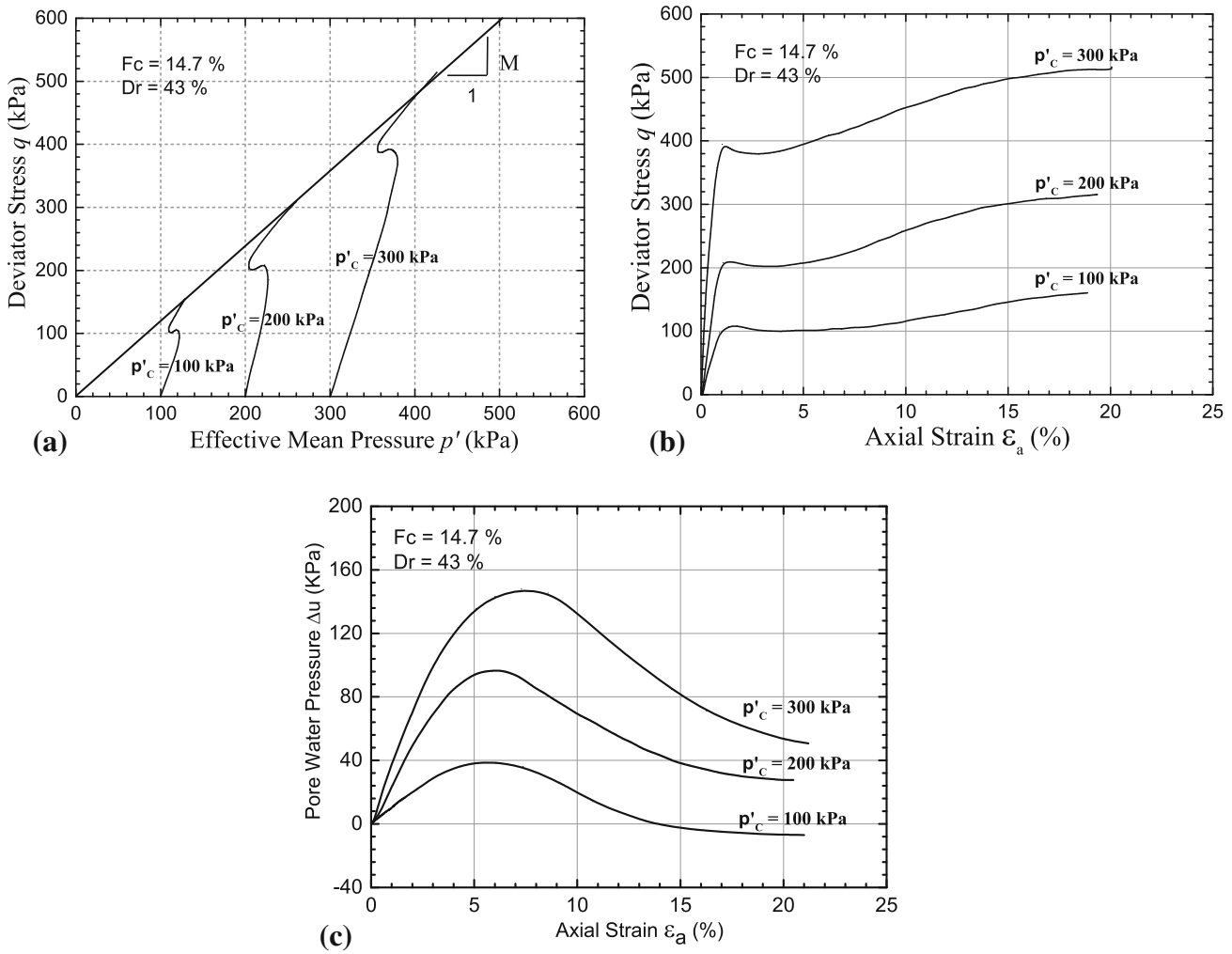

Fig. 9 Undrained compression test results on natural sand collected at 4 m depth for a confining mean stress of 100, 200 and 300 kPa

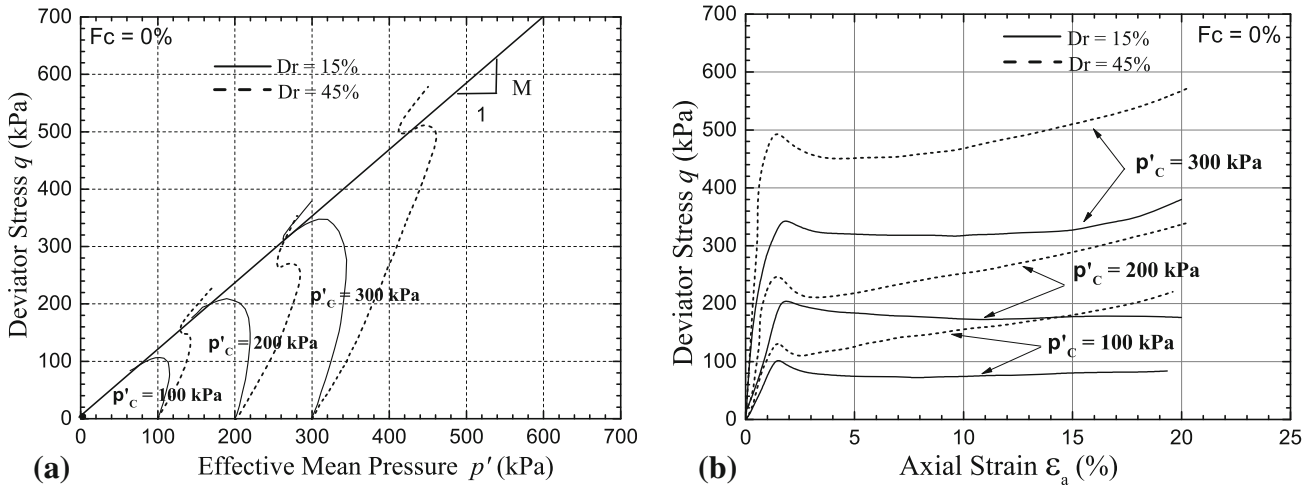

Fig. 10 Undrained triaxial compression test results for two initial relative densities ($D_r = 15$ and 45 %) at three levels of confining effective mean stresses ($p'_C = 100$, 200 and 300 kPa) of clean sand $F_C = 0\,\%$

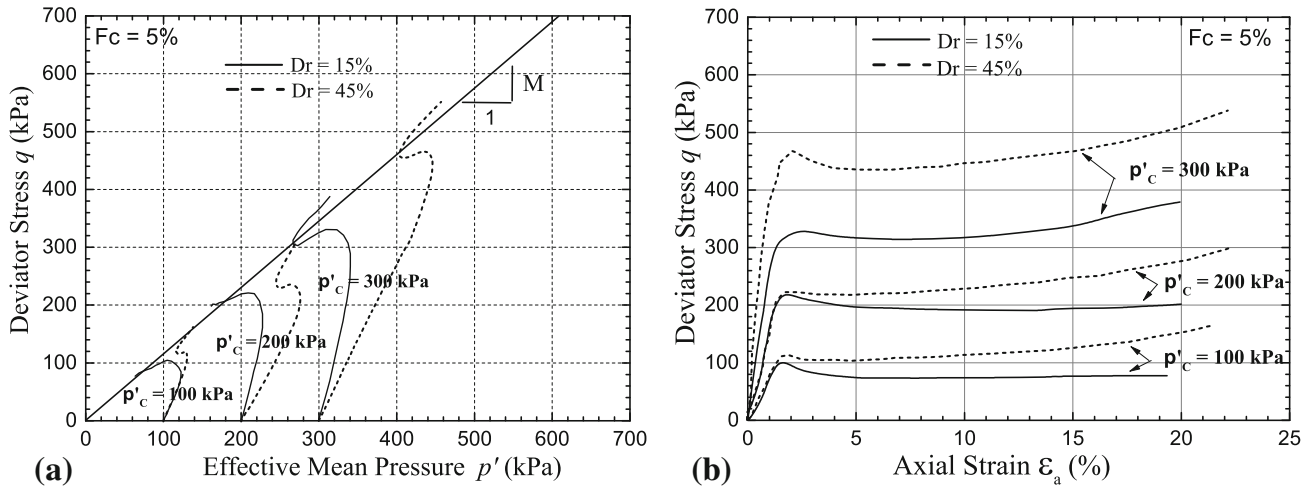

Fig. 11 Undrained triaxial compression test results for two initial relative densities ($D_r = 15$ and 45 %) at three levels of confining effective mean stresses ($p'_C = 100$ 200 and 300 kPa) of silty sand $F_C = 5$ %

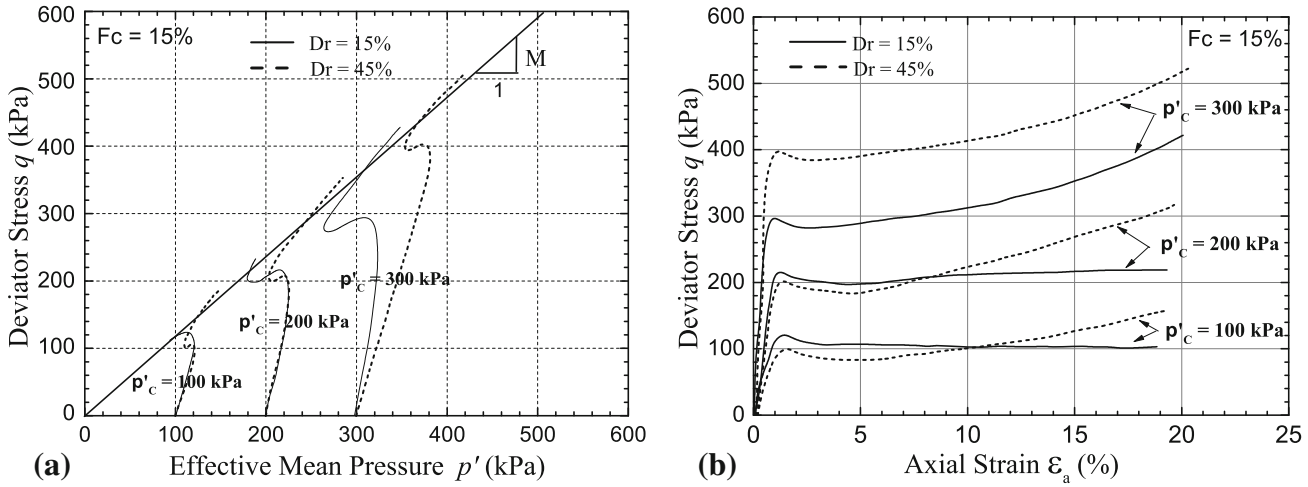

Fig. 12 Undrained triaxial compression test results for two initial relative densities ($D_r = 15$ and 45 %) at three levels of confining effective mean stresses ($p'_C = 100$, 200 and 300 kPa) of silty sand $F_C = 15$ %

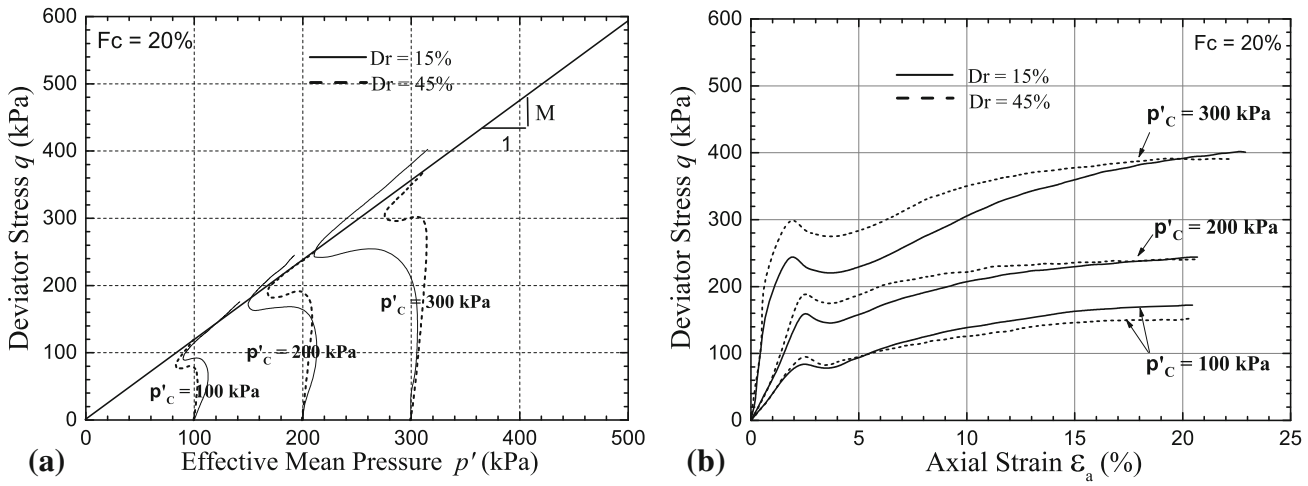

Fig. 13 Undrained triaxial compression test results for two initial relative densities ($D_r = 15$ and 45 %) at three levels of confining effective mean stresses ($p'_C = 100$, 200 and 300 kPa) of silty sand $F_C = 20$ %

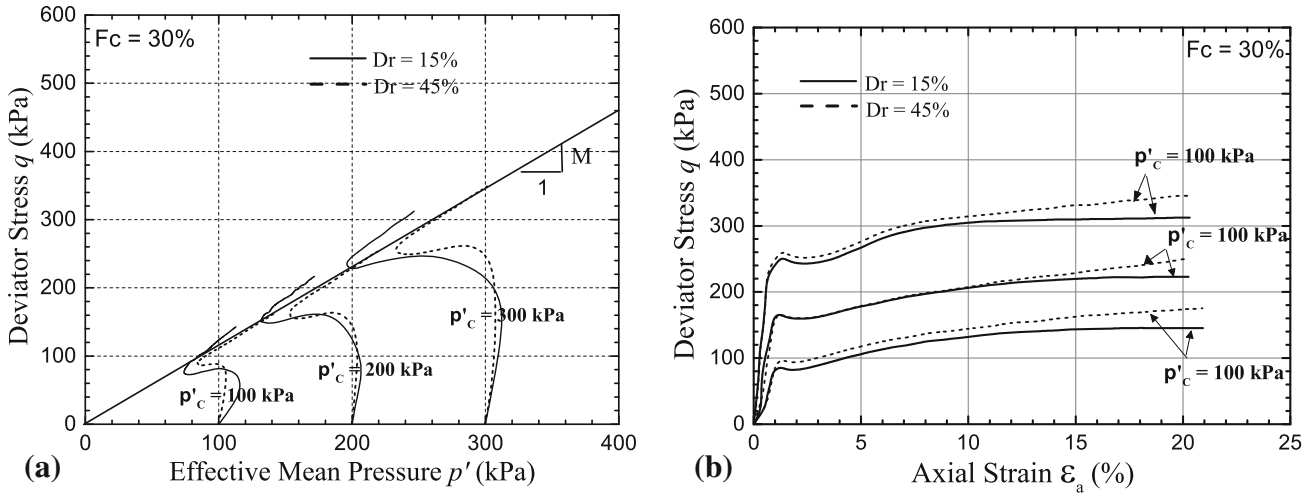

Fig. 14 Undrained triaxial compression test results for two initial relative densities ($D_r = 15$ and 45 %) at three levels of confining effective mean stresses ($p'_C = 100$, 200 and 300 kPa) of silty sand $F_C = 30\,\%$

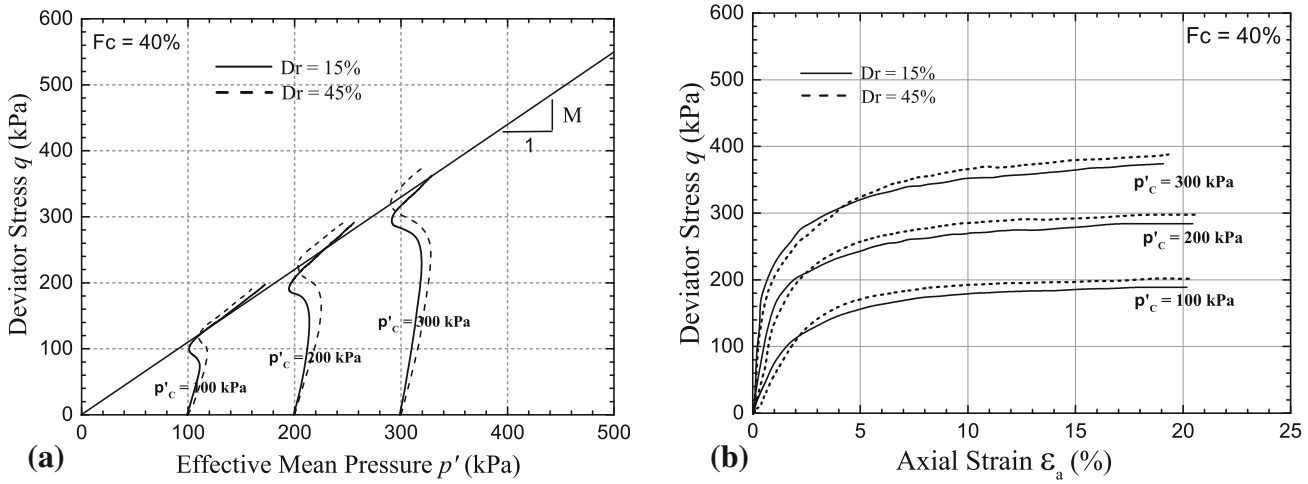

Fig. 15 Undrained triaxial compression test results for two initial relative densities ($D_r = 15$ and 45 %) at three levels of confining effective mean stresses ($p'_C = 100$, 200 and 300 kPa) of silty sand $F_C = 40\,\%$

to the role of the fines to increase the dilatancy in the soil mixtures. This shows that beyond 30 % of fine content, the fines participate in the strength of the mixture and reverse the behavior trend, and the mixture does not manifest instability neither liquefaction flow failure nor limited liquefaction. From laboratory test results, similar conclusions are reported by Pitman et al. [36], Thevanayagam and Mohan [37], Bobei and Wanatowski [38], Rahman and Lo [39].

Moreover, these results coincide with the actual observations in the three recent earthquakes, Northridge (1994), Kocaeli (1999) and Chi–Chi (1999), and all of these showed signs of liquefaction in soils with >15 % of fines. The same observations are noticed in the case of static liquefaction failure leading to catastrophic events reported by Kramer and Seed [40], Fourie and Tshabalala [41], in which post-liquefied soil has more than 20 % of silty fine content.

From the analysis of the obtained results, it can be seen that a relationship between initial relative density and normalized critical shear strength does exist in such a manner, increase in relative density results in increase in normalized critical shear strength. This relationship may enable the shear strengths of any sand specimen of a given initial relative density to be estimated, although the effect of sand type (particle size distribution, particle shape, mineralogy) would have to be taken into account. These latter properties are expressed in terms of critical state parameters in our analysis.

3.1 Effect of Low Plastic Fines on Critical State Parameters

The CSL of specified soil in ($e - \log p'$) and the (q, p') planes can be represented by a straight and unique line, under the condition that the soil is not subjected to modification of

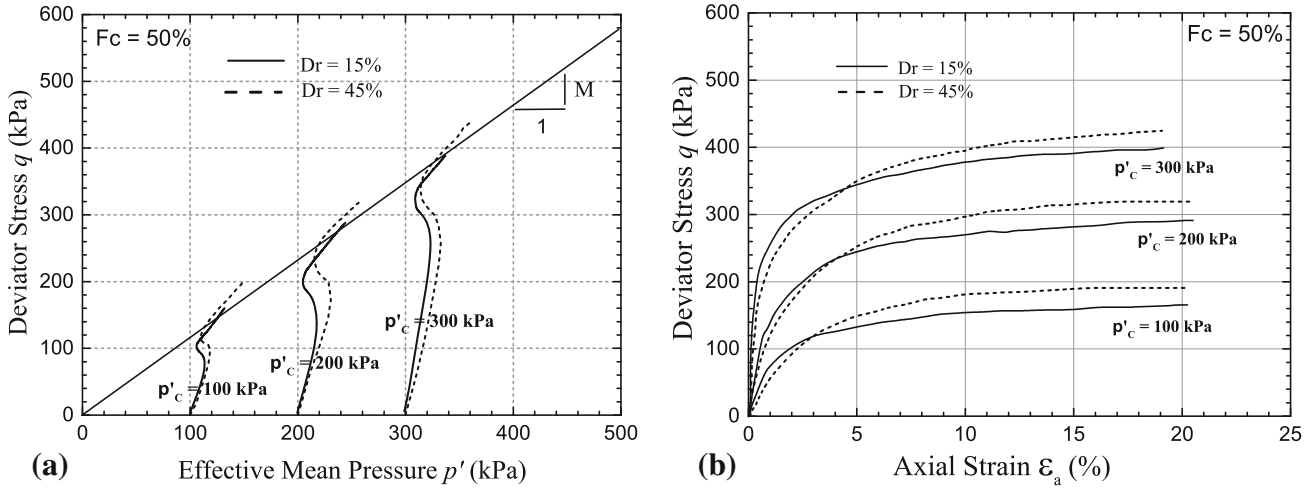

Fig. 16 Undrained triaxial compression test results for two initial relative densities ($D_r = 15$ and 45 %) at three levels of confining effective mean stresses ($p'_C = 100$, 200 and 300 kPa) of silty sand $F_C = 50$ %

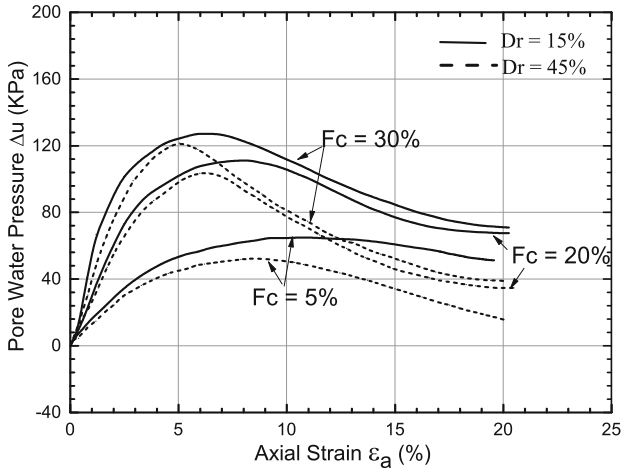

Fig. 17 Pore water pressure generation for two initial relative densities ($D_r = 15$ and 45 %) with different fine content at confining effective stress 200 kPa

grain size distribution (crushing of particle breakage) under applied stresses [27]. Uniqueness means that the CSL is not dependent on testing conditions such as sample preparation methods or strain rate.

It is essential to note that monotonic undrained behavior of sand–silt mixture is highly affected by initial conditions such as initial relative density state, global void ratio and confining effective mean stress.

When soil samples will be subjected to a state of continuous deformation with constant deviatoric stress (q) and effective mean stress (p') and when the shear strain is large, there exists a correlation between the void ratio at critical state and effective mean stress. The critical state line (CSL) is defined as the locus of all points within the void ratio – effective mean stress ($e - \log p'$) plane at which soil mass deforms under the conditions of constant stress and void ratio.

Before proceeding, it is useful to interpret the influence of fine silt content on liquefaction strength. It is more important to highlight how fine content affects the concepts of critical state of soil mechanics framework.

Results of the experimental tests of initial stress–density conditions and stress paths for a specified fine content fraction in both loading cases: drained and undrained and various initial relative densities fall along a unique CSL. By plotting the experimental data in ($e - \log p'$) plane, a linear equation for the CSL may be obtained by regression; such expression is already written as in Eq. (2).

The effect of silty fine content on critical undrained shear strength depends on the type of fine particles (particle shape, mineralogy and gradation properties) and initial relative density of the mixture. Fine particles influence instability susceptibility by modifying the critical state parameters as well as altering sand fabric shearing–compressibility characteristics and thus the critical undrained shear strength.

Based on the CSL, developed from results of drained triaxial compression tests carried out on loose and medium dense silty sand (initial relative densities 15 and 45 %) with fine content F_C ranging from 0 to 50 %, the critical state parameters λ_{CSL}, Γ_{CSL} and M are determined and analyzed.

Then, F_C, λ_{CSL}, Γ_{CSL} and M are correlated to obtain the following relationships:

$$\lambda_{CSL} = 0.0361 + 0.0773 F_C \quad (11)$$

$$\Gamma_{CSL} = 0.869 + 0.327 F_C \quad (12)$$

$$M = 1.246 + 0.12 F_C \quad (13)$$

Figure 18 shows the variation of the critical state parameters in terms of fine fraction. The shearing–compressibility λ_{CSL} of the mixture is a major parameter controlling the severity of the instability and thus the critical undrained shear

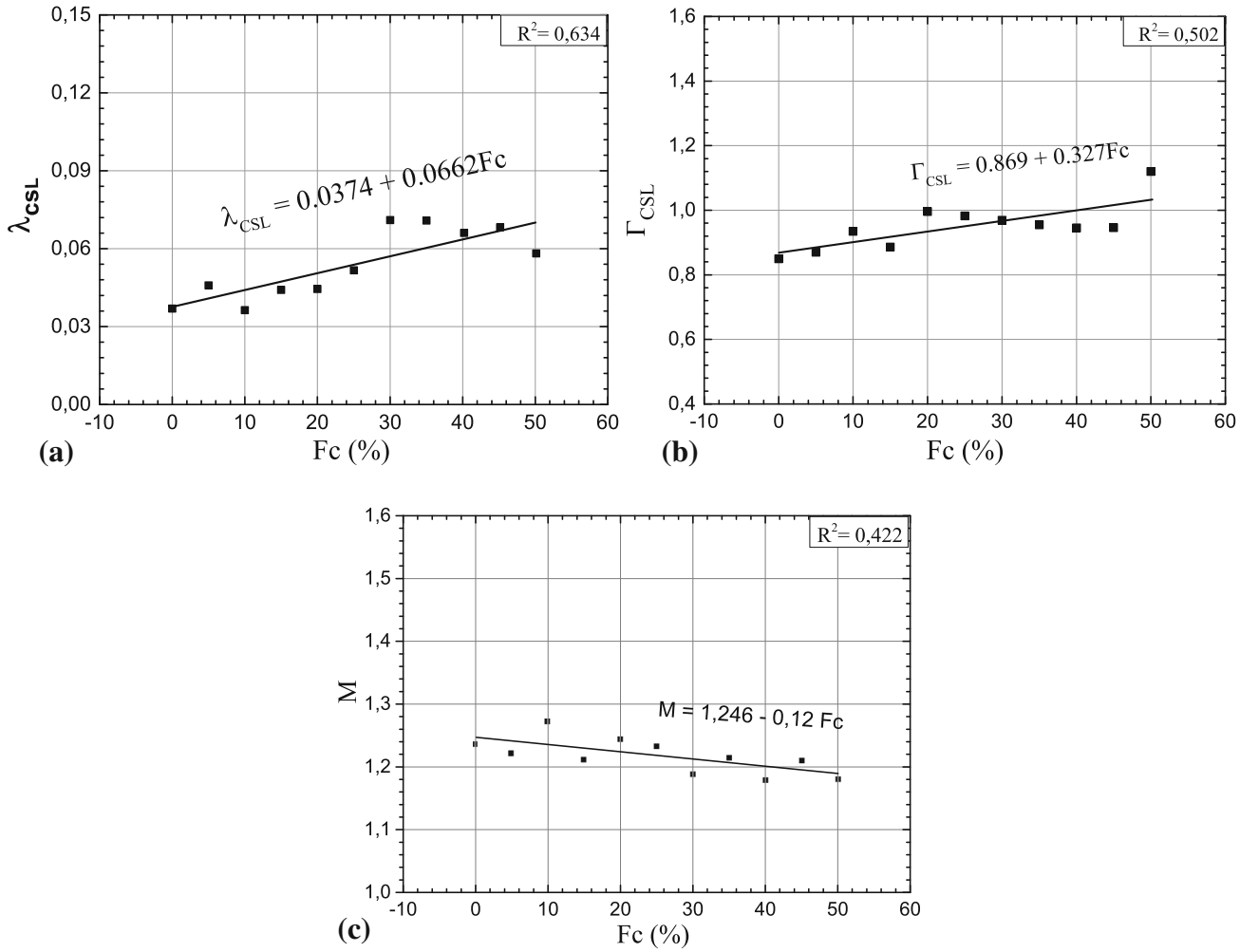

Fig. 18 Statistical evaluation of the effect of fine content on CSL parameters λ_{CSL}, Γ_{CSL} and M

strength. The slope of the λ_{CSL} may reveal the trend behavior of undrained shear strength in terms of fine content. Since the added silt belongs the parent sand (identical mineralogy), the CSL keeps more or less the same slope, and the effect of fine content on λ_{CSL} is not too significant, while Γ_{CSL} is dependent on mixture gradation characteristics and should vary in terms of fine content. In Fig. 19, Γ_{CSL} is correlated with λ_{CSL}, and a linear relationship is obtained as such:

$$\Gamma_{CSL} = 0.743 + 3.843\lambda_{CSL} \quad (14)$$

The experimental results show clearly that both parameters Γ_{CSL} and λ_{CSL} increase with the increase of fine content while M decreases smoothly with the increase of fine content as represented in Eq. (13) as follows:

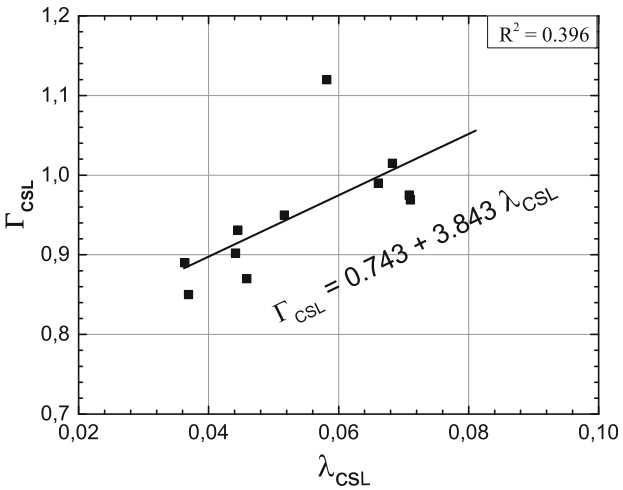

Fig. 19 Correlation between CSL parameters Γ_{CSL} and λ_{CSL}

3.2 Comparison Between Experimental Results and Results of Analytical Approach

The critical state parameters of reconstituted soil mixture specimens with different fine content are obtained in the previous section, and then, they are used for application in Eq. (10). Such equation is graphically represented in terms of ψ_{CSL} in Fig. 20, and ψ_{CSL} is not sufficient to describe the

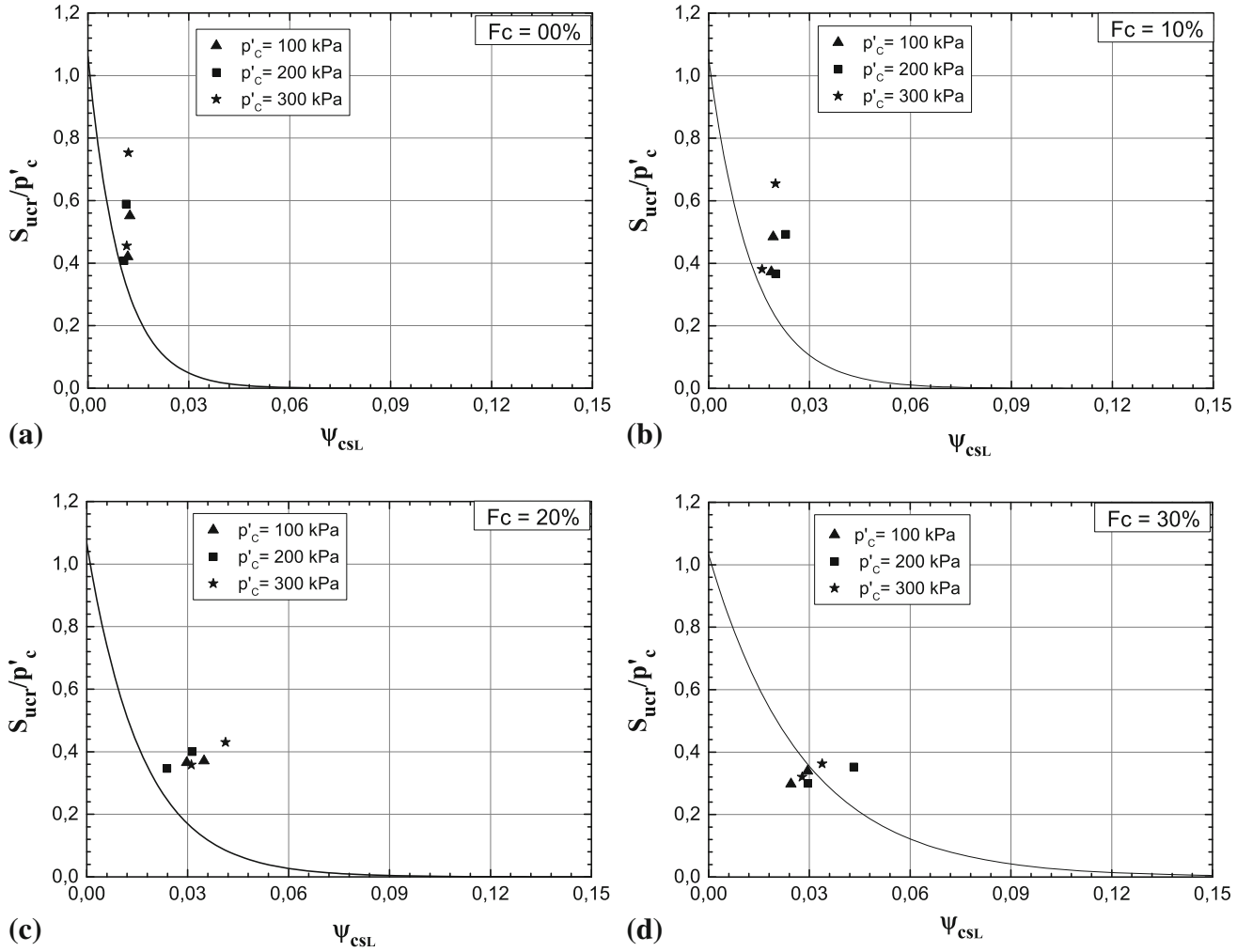

Fig. 20 Variation of normalized undrained critical shear strength S_{ucr}/p'_C versus state parameter ψ_{CSL} for different fine contents and for two initial relative density states ($D_r = 15\,\%$ and $D_r = 45\,\%$)

mechanical instability in undrained conditions (excess pore water pressure build-up in the mixture) without the shearing–compressibility property of the granular media. The latter controls the severity of strain softening and therefore the liquefaction vulnerability.

Adding fines till 30 % of the sand silt mixture makes the silty sand reaches critical state at smaller stresses. Increasing F_C would separate sand particles and consequently reduce the sand initial contact surfaces. Meanwhile, the strength of sand fabric of carrying loads becomes weaker and the critical state parameter increases with the increase of fine content leading to the reduction of normalized critical undrained shear strength. The results on undrained instability of silty sands having the same trend are discussed by Rahman and Lo [39] and Sadrekarimi [12].

Figure 20 shows the decreasing patterns of (S_{ucr}/p'_C) with increasing ψ_{CSL} for several F_C, and this behavior agrees with the compressibility property of silty sand under investigation. The variation of λ_{CSL} with F_C may be important in the trend of S_{ucr}/p'_C. Both parameters expressed in terms of a ratio $(\psi_{CSL}/\lambda_{CSL})$ should be included to estimate (S_{ucr}/p'_C), since e_{CSL} depends on λ_{CSL} and Γ_{CSL}. For both applications [analytical approach based on critical state parameters (Eq. 10) and experimental results], the behavior of the soil under investigation obeys to the same trend with regard to the variables under consideration. Meanwhile, the state variable ψ_{CSL} is the most important since it incorporates e_{CSL} which can be defined by both critical state parameters λ_{CSL} and Γ_{CSL}.

3.3 Effect of Grading Characteristics on Undrained Residual Shear Strength

Table 2 contains the results of residual shear strengths related to grading characteristics and fine content. The analysis is limited for the range of fine content [0–50 %].

Table 2 Residual shear strengths with grading characteristics and fine content ($p'_c = 300$)

Material	F_C (%)	D_{50} (mm)	C_u	C_c	D_r (%)	ϕ_S (°)	S_{ucr}/P'_c	Observation
Clean sand	0	0.339	1.704	1.073	15	30.83	0.45	Contractive/dilative
					45	32.06	0.63	
Silty sand	5	0.331	1.983	1.194	15	30.50	0.45	Contractive/dilative
					45	30.73	0.62	
Silty sand	15	0.317	32.303	16.558	15	30.27	0.40	Contractive/dilative
					45	30.44	0.55	
Silty sand	20	0.307	37.102	16.441	15	31.01	0.31	Contractive/dilative
					45	30.85	0.39	
Silty sand	30	0.283	41.797	3.418	15	29.75	0.35	Contractive/dilative
					45	29.79	0.36	
Silty sand	40	0.242	43.421	0.063	15	29.54	0.54	Dilative
					45	29.13	0.57	
Silty sand	50	0.076	41.424	0.063	15	29.58	0.61	Dilative
					45	29.51	0.58	

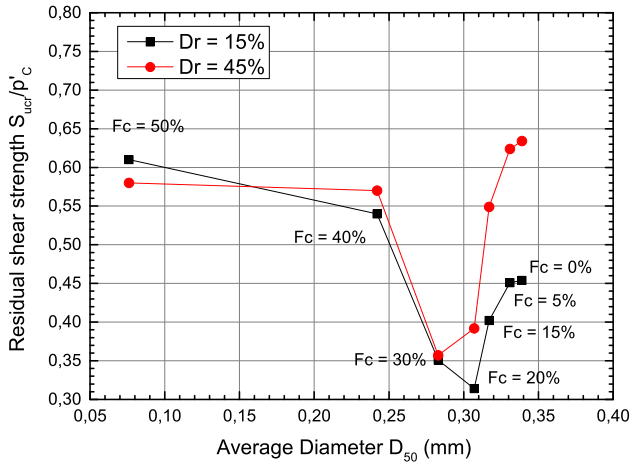

Fig. 21 Variation of residual shear strength with D_{50} and fine content F_c

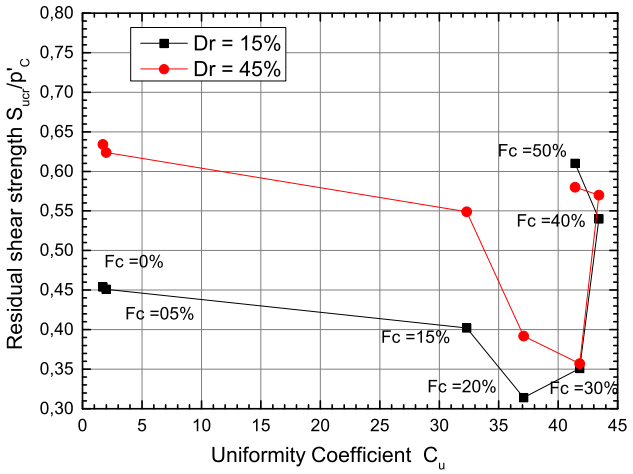

Fig. 22 Variation of residual shear strength with C_u and fine content F_c

3.3.1 Effect of Median Diameter D_{50}

Figure 21 shows a decrease of residual shear strength with a decrease of median diameter D_{50} and an increase of fine content F_c until a value of fine content falling within the range of 20 and 30 %. Beyond these values, the residual strength tends to increase with an increase of fine content. We can observe for both relative densities, i.e., 15 and 45 %, a convergence of residual shear strength values for high values of fine content. This behavior may be interpreted as that the increase in fine content may induce contracting behavior of silt–sand mixture.

3.3.2 Effect of Uniformity Coefficient C_u and Coefficient of Curvature C_c

The effect of uniformity coefficient C_u on the mechanical behavior of the specimens is shown in Fig. 22. It can be seen that the undrained residual shear strengths S_{ucr} decrease as the coefficient of uniformity and fine content decreases up to values of 20 and 30 % of fine content. Beyond these values, the trend of residual strength is reversed.

Figure 23 shows that the residual shear strength decreases with the increase of the coefficient of gradation up to 15 % fine content; beyond that, it decreases sharply with a very slight decrease of the coefficient of gradation up to 20 % fine content, where it increases with increasing of the coefficient of gradation.

4 Conclusions

Numerous studies reported in the literature have produced varying answers to the question about the effect of increasing fine content on liquefaction behavior of sandy soils. In the present paper, an experimental investigation has been per-

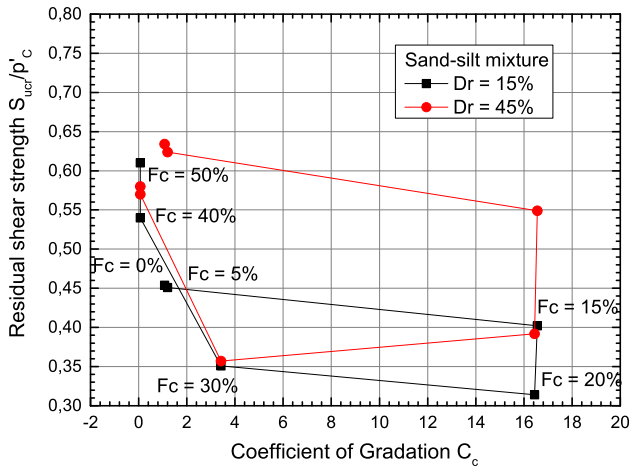

Fig. 23 Variation of residual shear strength with C_c and fine content F_c

formed as an attempt to answer to this question. A series of monotonic undrained triaxial tests were carried out on natural samples and on reconstituted saturated sand–silt mixtures specimens with specified content of fine fraction ranging from 0 to 50 % under two combinations of initial relative densities (15 and 45 %). The samples were isotropically consolidated at three levels of confining effective mean stresses (100, 200 and 300 kPa). The sand under investigation was collected from coastal region of Mostaganem site where an extensive urban project is planned. Moreover, it lies on geological layers of vast deposits of saturated silica sand vulnerable to mechanical instability.

The results analysis was made in the context of critical state soil mechanics concepts and liquefaction susceptibility of sands. The major conclusions of the present study can be drawn as follows:

1 Two distinct stress path tendencies have been shown in this study. Loose samples show amplified contractive phase, while medium dense samples exhibit a contractive phase followed by a dilative phase in undrained conditions.
2 The relationship between the normalized critical shear strength and the initial relative density may enable the shear strengths of any sand specimen with a given initial relative density to be estimated, although the effect of sand type (particle size distribution, particle shape, mineralogy) would have to be taken into account. An attempt to express these properties in terms of critical state parameters has been done with success in our analysis.
3 Up to 30 % of fine content, in loose and medium dense states, Mostaganem sand is susceptible to limited liquefaction.
4 The state parameter ψ_{CSL} is not sufficient to describe the mechanical instability in undrained conditions (development of pore water pressure in the mixture) of silty sands without the shearing–compressibility property of the granular media. The latter controls the severity of strain softening and therefore the liquefaction vulnerability.
5 The obtained expression of the undrained critical shear strength via critical state of soil mechanics concept depends on initial state of the soil and the critical state parameters.
6 Increasing fine content would separate sand particles and consequently reduce the sand initial contact surfaces. Meanwhile, the strength of sand fabric of carrying loads becomes weaker and the critical state parameter increases with the increase in fine content leading to the reduction of normalized critical undrained shear strength.
7 The liquefaction resistance of sand–silt mixtures may either decrease or increase with increasing values of fine content, indicating the existence of a threshold value of fine content of 30 %.
8 Undrained residual shear strengths decrease as the average diameter D_{50} decreases and fine content increases up to 30 %. This phenomenon is explained by the fact that, when fine content increases in the range of 0–30 %, the fine particles of silt are positioned among the sand grains, changing the structure of sand and consequently decreasing the void ratio. This will decrease the undrained residual shear strength S_{ucr}. It was observed that the trend is reversed beyond the value of fine content of 30 %.
9 A similar trend as for average diameter D_{50} can be seen for the variation of undrained residual shear strength S_{ucr} with uniformity and curvature coefficients.
10 The critical state parameters may replace the soil shape property, mineralogy, fraction of fine content in evaluating the severity of instability, while confining pressure and initial relative density may indicate the susceptibility to soil instability under undrained conditions.

It is acknowledged that the above outcome is based on limited tests data and must be completed by a cyclic triaxial test results. The influence of low plastic fine content on the critical state line of silty sand soils needs to be characterized furthermore taking into account particle size distribution, particle shape and soil mineralogy.

References

1. Idriss, I.M.; Boulanger, R.W.: Soil Liquefaction During Earthquakes. Earthquakes Engineering Research Institut (EERI), Oakland (2008)
2. Lenart, S.; Koseki, J.; Miyashita, Y.: A soil liquefaction in the tone river basin during the 2011 earthquake of the pacific coast of Tohoku. Acta Geotech. Slov. **9**(2), 5–15 (2012)

3. Eskisar, T.; Karakan, E.; Altun, S.: Evaluation of cyclic stress–strain and liquefaction behavior of Izmir sand. Arab. J. Sci. Eng. **39**, 7513–7524 (2014). doi:10.1007/s13369-014-1312-3
4. Olson, S.M.; Stark, T.D.: Yield strength ratio and liquefaction analysis of slopes and embankments. J. Geotech. Geoenviron. Eng. **129**(8), 727–737 (2003). doi:10.1061/(ASCE)1090-0241(2003)129:8(727)
5. Belkhatir, M.; Schanz, T.; Arab, A.; Della, N.: Experimental study on the power water pressure generation characteristics of saturated silty sands. Arab. J. Sci. Eng. **39**, 6055–6067 (2014). doi:10.1007/s13369-014-1238-9
6. Troncoso, J.H.; Verdugo, R.: Silt content and dynamic behavior of tailing sands. In: Proceedings of the XI International Conference on Soil Mechanics and Foundation Engineering, pp. 1311–1314 (1985)
7. Vaid, Y.P.: Liquefaction of silty soils. In: Prakash, S., Dakoulas, P. (eds.) Ground Failures under Seismic Conditions, pp. 1–16. Geotechnical special publication no. 44. American Society of Civil Engineers, New York (1994)
8. Thevanayagam, S.: Effect of fines and confining stress on undrained shear strength of silty sands. J Geotech. Geoenviron. Eng. **124**(6), 479–490 (1998)
9. Missoum, H.; Belkhatir, M.; Bendani, K.; Maliki, M.: Laboratory investigation into the effects of silty fines on liquefaction susceptibility of Chlef (Algeria) sandy soils. J. Geotech. Geol. Eng. **31**(1), 279–296 (2013). doi:10.1007/s10706-012-9590-6
10. Wang, W.S.: Some Findings in Soil Liquefaction. Water Conservancy and Hydroelectric Power Scientific Research Institute, Beijing (1979)
11. Prakash, S.; Puri, V.K.: Recent advances in liquefaction of fine grained soils. In: 5th International Conference on Recent Advances in Geotechnical Earthquake Engineering and Soil Dynamics, San Diego, CA, pp. 1–6 (2010)
12. Sadrekarimi, A.: Influence of fines content on liquefied strength of silty sands. Int. J. Soil Dyn. Earthq. Eng. **55**, 108–119 (2013). doi:10.1016/j.soildyn.2013.09.008
13. Yamamuro, J.A.; Lade, PV.: Steady-state concepts and static liquefaction of silty sands. J. Geotech. Geoenviron. Eng. **124**(9), 868–877 (1998). doi:10.1061/(ASCE)1090-0241(1998)124:9(868)
14. Seed, H.B.; Idriss, I.M.; Arango, I.: Evaluation of liquefaction potential using field performance data. J. Geotech. Geoenviron. Eng. **109**(3), 458–482 (1983). doi:10.1061/(ASCE)0733-9410(1983)109:3(458)
15. Stark, T.D.; Mesri, G.: Undrained shear strength for liquefied sands for stability analysis. J. Geotech. Eng. **118**(9), 1727–1747 (1992)
16. Olson, S.M.; Stark, T.D.: Liquefied strength ratio from liquefaction flow failure case histories. Can. Geotech. J. **39**, 629–647 (2002). doi:10.1139/t02-001
17. Yamamuro, J.A.; Kelly, M.C.: Monotonic and cyclic liquefaction of very loose sands with high silt content. J. Geotech. Geoenviron. Eng. **127**(4), 314–324 (2001). doi:10.1061/(ASCE)1090-0241(2001)127:4(314)
18. Maheshwari, B.K.; Patel, A.K.: Effects of non-plastic silts on liquefaction potential of Solani sand. Geotech. Geoenviron. Eng. **28**(5), 559–566 (2010). doi:10.1007/s10706-010-9310-z
19. ASTM, D2487-11.: Standard Practice for Classification of Soils for Engineering Purposes (Unified Soil Classification System). ASTM International, West Conshohocken (2011). doi:10.1520/D2487-11
20. Missoum, H.; Belkhatir, M.; Bendani, K.: Undrained shear strength response under monotonic loading of Chlef (Algeria) sandy soil. Arab. J. Geosci. **6**, 615–623 (2013). doi:10.1007/s12517-011-0387-3
21. Ladd, R.S.: Specimen preparation and liquefaction of sands. J. Geotech. Eng. Div. **100**(10), 1180–1184 (1974)
22. Mulilis, J.P.; Arulanandan, K.; Mitchell, J.K.; Chan, C.K.; Seed, H.B.: Effects of sample preparation on sand liquefaction. J. Geotech. Eng. Div. **103**(2), 91–108 (1977)
23. Vaid, Y.P.; Sivathayalan, S.; Stedman, D.: Influence of specimen-reconstituting method on the undrained response of sand. ASTM Geotech. Test. J. **22**(3), 187–195 .refdoc.fr/Detail notice?idarticle=11381016 (1999)
24. ASTM, D4767-02.: Standard Test Method for Consolidated Undrained Triaxial Compression Test for Cohesive Soils, vol. 04.08, pp. 1–13. American Society for Testing and Materials, West Conshohocken (2004). doi:10.1520/D4767-02
25. Poulos, S.J.: The steady state of deformation. J. Geotech. Eng. **107**(5), 553–562 (1981)
26. Been, K.; Jefferies, M.G.; Hachey, J.: The critical state of sands. Géotechnique **41**, 365–381 (1991)
27. Kramer, S.L.; Wang, C.H.; Byers, M.B.: Experimental measurement of the residual strength of particulate materials. In: Lade, P.V.; Yamamuro, J.A. Physics and Mechanics of Soil Liquefaction, pp. 249–259. Balkema, Rotterdam (1999)
28. Been, K.; Jefferies, M.A.: state parameter for sands. Géotechnique **35**, 99–112 (1985). doi:10.1680/geot.1985.35.2.99
29. Schofield, A.; Wroth, P.: Critical State Soil Mechanics. McGraw-Hill, London (1968)
30. Shen, C.K.; Vrymoed, J.L.; Uyeno, C.K.: The effect of fines on liquefaction of sands. In: 9th International Conference on Soil Mechanics and Foundation Engineering, pp. 281–285 (1977)
31. Troncoso, J.H.; Verdugo, R.: Silt content and dynamic behavior of tailing sands. In: Proceedings of the XI International Conference on Soil Mechanics and Foundation Engineering, pp. 1311–1314 (1985)
32. Sladen, J.A.; D'Hollander, R.D.; Krahn, J.; Mitchell, D.E.: Back analysis of the Nerlerk berm liquefaction slides. Can. Geotech. J. **22**, 579–588 (1985)
33. Koester, J.P.: The influence of fines type and content on cyclic strength. In: Prakash, S., Dakoulas, P. (eds.) Ground Failures Under Seismic Conditions, pp. 17–33. ASCE, New York (1994)
34. Naeini, S.A.; Baziar, M.H.: Effect of fines content on steady-state strength of mixed and layered samples of a sand. Soil Dyn. Earthq. Eng. **24**, 181–187 (2004). doi:10.1016/j.soildyn.2003.11.003
35. Kokusho, T.; Nagao, Y.; Ito, F.; Fukuyama, T.: Sand liquefaction observed during recent earthquake and basic laboratory studies on aging effect. In: Maugeri, M., Soccodato, C. (eds.) Earthquake Geotechnical Engineering Design, pp. 75–92. Springer, Switzerland (2014). doi:10.1007/978-3-319-03182-8_3
36. Pitman, T.D.; Robertson, P.K.; Sego, D.C.: Influence of fines on the collapse of loose sands. Can. Geotech. J. **31**(5), 728–739 (1994). doi:10.1139/t94-084
37. Thevanayagam, S.; Mohan, S.: Intergranular state variables and stress–strain behavior of silty sands. Geotechnique **50**(1), 1–23 (2000). doi:10.1680/geot.2000.50.1.1
38. Bobei, D.C.; Wanatowski, D.: Modified state parameter for characterizing static liquefaction of sand with fines. Can. Geotech. J. **46**(3), 281–295 (2009). doi:10.1139/T08-122
39. Rahman, M.M.; Lo, S.R.: Predicting the onset of static liquefaction of loose sand with fines. J. Geotech. Geoenviron. Eng. **138**(8), 1037–1041 (2012). doi:10.1061/(ASCE)GT.1943-5606.0000661
40. Kramer, S.L.; Seed, H.B.: Initiation of soil liquefaction under static loading conditions. J. Geotech. Geoenviron. Eng. **114**(4), 412–430 (1988). doi:10.1061/(ASCE)0733-9410(1988)114:4(412)
41. Fourie, A.B.; Tshabalala, L.: Initiation of static liquefaction and the role of K_0 consolidation. Can. Geotech. J. **42**(3), 892–906 (2005). doi:10.1139/t05-026